

The Development of the Velocity Field in Polymer Melts in a Reservoir Approaching a Capillary Die

TIMOTHY F. BALLENGER and JAMES L. WHITE, *Department of Chemical and Metallurgical Engineering, University of Tennessee, Knoxville, Tennessee 37916*

Synopsis

Color motion pictures have been made of the flow of low-density polyethylene, polystyrene, and isotactic polypropylene at 180°C in the reservoir approach to a capillary extrusion rheometer. Detailed observations of the variation of flow patterns with extrusion rate were made. At low flow rates, essentially radial flow into the capillary entrance was observed in all polymers. With increasing flow rate, the included entrance angle α for the polyethylene and polystyrene decreased from 180°C and a "wine glass" structured velocity field was observed with stagnant circulating regions in the corners and the melt channeling in through the wine glass to the capillary entrance. The angle α was related to entrance pressure drop Δp_e and capillary wall shear stress σ_w data through the semilogarithmic equation

$$\alpha = 178.5(0.9644)^{\Delta p_e/\sigma_w}$$

where α is in degrees; $\Delta p_e/\sigma_w$ is interpreted as a Weissenberg number. The breakdown of stable laminar flow of the melts in the reservoir and the distortion of extrudates was observed. These phenomena seemed to be initiated by the formation of a spiralling motion in the reservoir.

INTRODUCTION

The character of velocity fields in polymer melts during processing operations is of considerable technological interest and importance. Perhaps the most important of all geometries for study is the entrance region to capillary dies, for it has long been realized that the distortion of emerging extrudates is closely related to the flow and stress fields in this region.¹⁻⁶ The earliest experiments on flow visualization in this geometry were published by Tordella³ on low-density polyethylene in 1957. In succeeding years, various other groups of researchers⁴⁻⁶ published improved experimental studies for flow of both low-density and the newer high-density polyethylenes. After several years of lagging interest, a number of researchers have since the late 1960's returned to this problem. Giesekus⁷ and Schummer⁸ have studied entrance profiles in polyacrylamide and polyisobutylene solutions, den Otter⁹ has investigated silicones, and the present authors^{10,11} have studied a wide range of polymer melts including polyethylene, polystyrene, isotactic polypropylene, poly(methyl methacrylate), and a polyisobutylene solution.

Tordella and other early researchers generally observed the flow patterns over only a limited range of flow rates and found in low-density polyethylene a velocity field differing significantly from that predicted¹² and observed¹³ in low molecular weight Newtonian fluids. Large circulating regions were observed in the corners of the entry reservoir, and the melt moved into the capillary through a funnel-shaped region (see Fig. 1). The later investigation of Bagley and Birks⁴ on high-density polyethylene showed, in marked contrast to this, a flow radially inward from the reservoir to the capillary as found in Newtonian fluids. Den Otter's observation on silicones showed a similar contrast between one melt which resembled low-density polyethylene and a second whose response was similar to a Newtonian fluid. Our own results indicated that different polymer melts and solutions exhibit a wide range of entrance flow patterns varying from that of a Newtonian

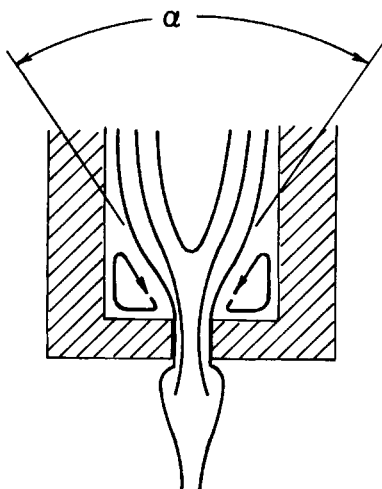


Fig. 1. Entrance flow patterns.

fluid to patterns with flows possessing larger secondary circulating flows than did low-density polyethylene in the various reports of its behavior. The careful and well-thought-out experiments of Giesekus⁶ have looked at the variation of two-dimensional entrance flow patterns in polyacrylamide and polyisobutylene as extrusion rate is increased. This researcher found that, at low flow rates, the solutions flowed radially from a reservoir into a die and that, at higher flow rates, the circulating flows develop in the corner regions, their size increasing as flow rate increases.

The breakdown of this entrance velocity field and its relationship to the distortion of emerging extrudates of low-density polyethylene was first pointed out by Tordella, and later authors^{2-6,14} have elaborated on this behavior. The present authors¹⁰ have made similar observations on polystyrene melts and have reported, as has Giesekus,⁷ the development of

instabilities in polyisobutylene and polyacrylamide solutions.* A detailed comparison, however, of the physical mechanisms of instability that have been proposed in the literature shows contradiction (see Bialas and White²).

It is the purpose of this paper to describe an experimental study¹⁸ of the variation in the capillary entrance flow patterns of three polymer melts (low-density polyethylene, polystyrene, and isotactic polypropylene) over a wide range of flow rates. The development of the flow patterns and the instability is described. A correlation between the flow patterns of these and other melts and their rheological properties is presented.

EXPERIMENTAL

Procedure

The flow studies were carried out in the reservoir of an Instron capillary rheometer which consists of a barrel $\frac{3}{8}$ in. wide and $12\frac{3}{4}$ in. long.^{18,19} Flow visualization was accomplished through the use of a heated glass extension to the rheometer barrel. The glass used was heavy-wall Pyrex tubing ($\frac{19}{32}$ in. outer diameter and $\frac{3}{32}$ in. wall) ordered from *Scientific Glass Apparatus Company* and cut into $\frac{7}{8}$ in. lengths. The lengths were sealed in a carbon steel heater frame between Teflon gaskets which were compressed when the capillary die was tightened up against the glass. Heat was generated by four General Electric 75-watt tubular heaters placed symmetrically in and along the entire length of the frame. The entrance region was photographed through a $\frac{7}{16}$ in. \times $\frac{5}{8}$ in. window in the frame which was enclosed by an insulator composed of Fiberglas encased in aluminum sheet outside and RTV silicone adhesive inside. The temperature of the glass extension was measured with an iron-Constantan thermocouple and controlled manually with a Powerstat to regulate the voltage of the heaters.

Motion pictures were taken of the steady-state entrance flow patterns using a Traid Model 70 motion picture camera, clutch driven by a 1.8-ampere Bell and Howell motor and mounted on a tripod in front of the Instron. Light was transmitted from the back of the heater frame by a 100-watt high-intensity lamp dispersed through a ground-glass prism placed in the window opposite the camera.

* The distortion of jets of polymer solutions emerging from spinnerets at high velocities in laminar flow has apparently long been known, worried about, utilized, and avoided by commercial operators of dry-spinning processes.¹⁵ This sort of behavior was long unknown to academic and many industrial researchers in polymer solution rheology. Investigators of the nature of capillary jets of polymer solutions have missed observing this phenomenon because of a tendency to use long capillary tubes.¹⁶ The distortion phenomenon was first pointed out to one of the authors (JLW) by Prof. R. Shinnar of City College who had seen it in a series of experiments. This was later mentioned in a publication by him and his colleagues.¹⁷ The situation was clarified by the researches of Giesekus.⁷ The present authors have confirmed Giesekus' work in a modified geometry.

The polymer samples were obtained in the form of $3/8$ -in.-diameter rods. These rods were first cut into 10-in. lengths, then 0.041-in.-diameter holes were drilled parallel to each other, normal to, and in a plane containing the longitudinal axis (compare Bagley and Birks⁶). Spacing between the holes ranged between $1/8$ and $1/4$ in. When the holes had been drilled, the outside diameter along the entire length of the rod was ground down to fit the Instron barrel. Since the extension had a larger diameter, the bottom of the rod was not ground. The rods were marked for melt flow visualization by inserting 0.035-in.-diameter colored threads of the same polymer into the holes. The threads had been separately extruded and then colored with red, green, blue, and brown Magic Markers.

The rod-colored thread composite was then inserted into the bottom of the Instron and rotated until the plane of marking threads was aligned with a line drawn normal to the line of sight on the bottom of the furnace. The heater frame was then screwed onto the Instron barrel and the plunger inserted. Heating to a temperature of $180^{\circ}\text{C} \pm 0.5^{\circ}\text{C}$ was carried out under a pressure of 20 to 30 psi, and the system and thermal equilibrium were reached in about 20 min. At this point, extrusion was begun by setting the plunger speed to 0.005 in./min. When the force response reached a steady state, 7 to 8 ft of motion picture film was taken at 16 frames/sec. This procedure was repeated at higher flow rates. At the first suspicion, however, of departures from smooth laminar flow the camera was turned on without waiting for a steady state to be achieved. Entrance patterns were photographed at each flow rate until the bursting pressure of the glass tube was reached (usually between 2500 and 3000 psi).

Materials

Several attempts to mold pellets of different polymers into rods were unsuccessful because of the formation of bubbles. Therefore, commercially available rods were purchased from the Cadillac Plastics and Chemical Company (Louisville, Kentucky).

Three polymers* were used in this study whose characteristics may be described as follows:

Low-Density Polyethylene. This polymer, which had a room temperature density of 0.910 g/cm^3 , was further characterized by measurement in the Instron rheometer¹⁹ viscosity μ , shear rate Γ , relationship at the temperature of the flow visualization study (180 C). This is plotted in Figure 2. The capillary entrance pressure drop, Δp_e , was determined from the intercept of the graph of total pressure versus capillary length/diameter ratio.¹⁹ Figure 3 is a plot of the entrance pressure drop Δp_e reduced with

* A limited number of experiments were carried out using nylon 66 rod obtained from the same supplier. The flow field seemed to be approximately radially inward to the capillary entrance, indicating probably smaller stagnant regions than described in our earlier paper.¹⁰ One interesting observation in the few nylon 66 experiments was the collection of nearly stationary air bubbles near the capillary entrance—apparently the Uebler effect as described by Metzner.²⁰

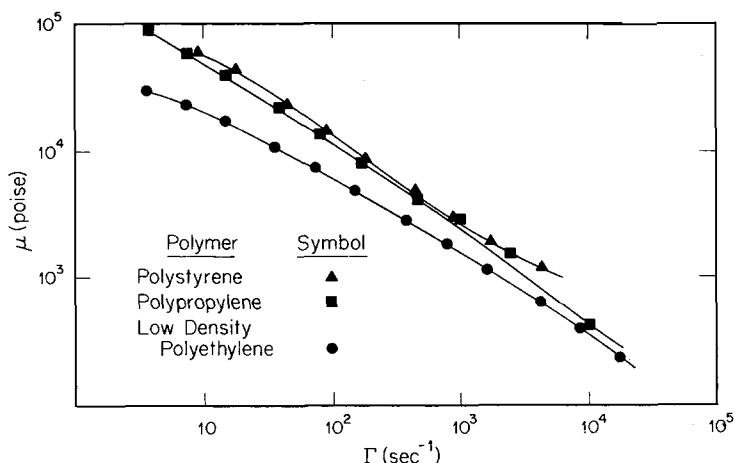


Fig. 2. Non-Newtonian shear viscosity of polymer melts studied as a function of shear rate. $T = 180^{\circ}\text{C}$.

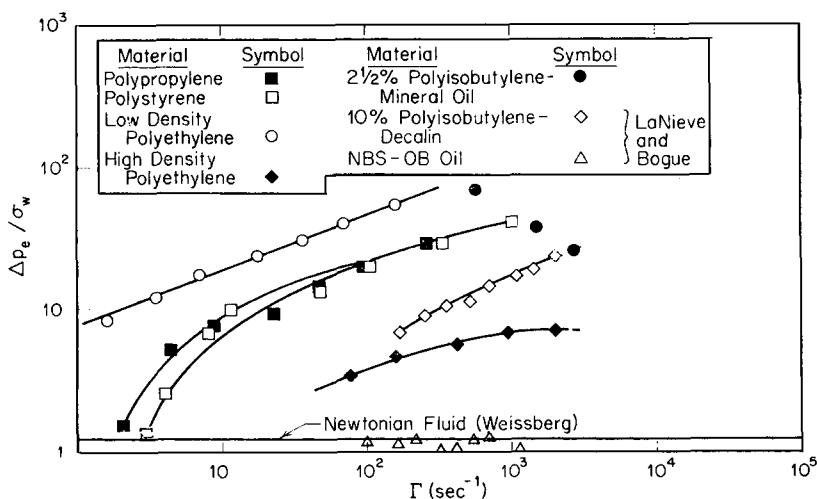


Fig. 3. Plot of entrance pressure drop reduced with the shear stress as a function of shear rate.

the capillary wall shear stress σ_w . Since Δp_e has been found to be, if not proportional to the principal normal stress difference $(\sigma_{11} - \sigma_{22})$ evaluated at the capillary die wall, a monotonic increasing function of it,^{21,22} Figure 3 may be interpreted as a plot of this capillary wall principal normal stress difference divided by the shearing stress versus shear rate.¹¹

Polystyrene. This is an atactic glassy polymer having a room temperature density of 1.05 g/cm³. D. G. Salladay of our group has determined its molecular weight distribution by gel permeation chromatography. This gives an M_n of 1.1×10^5 and an M_w of 3.1×10^5 , with M_w/M_n being

2.82. The viscosity at 180°C is plotted versus shear rate in Figure 2, and $\Delta p_e/\sigma_w$ versus shear rate in Figure 3.

Polypropylene. This is an isotactic polymer with a room temperature of 0.90 g/cm³. The viscosity data at 180°C are plotted in Figure 2, and $\Delta p_e/\sigma_w$ in Figure 3. For purposes of comparison data on Newtonian fluids, high-density polyethylene and polymer solutions are also given in Figure 3.

RESULTS

Low-Density Polyethylene

At low flow rates, this melt seemed to flow almost radially inward into the capillary, as is done by a Newtonian fluid.¹³ (See Fig. 4.) However, as the flow rate was increased, the entrance angle α seemed to continually decrease from an initial value near 180° to 90° and indeed smaller values. Coupled with the development of this wine glass stem capillary approach pattern was the development of circulating secondary flows in the bottom corners of the reservoir. As the flow rate increased, the size of these secondary flow regions correspondingly increased. Figure 5 is a plot of the angle α as a function of capillary wall shear rate.

At a capillary wall shear rate of 66 sec⁻¹ a slight swirling motion was observed in the inlet. (The swirling oscillation has the superficial appearance of a bathtub-like vortex, but, instead of the expected bulk rotation, the centermost flow line seems to simply revolve about the centerline tracing out a circular path at the capillary inlet. The distinction is subtle but necessary to distinguish the two types of motion.) The emerging extrudate, which had been smooth at lower flow rates, remained smooth.

At the next change in flow rate (to a capillary wall shear rate of 154 sec⁻¹, the slight oscillation became somewhat more vigorous, and the colored core of the extrudate began to assume the foam of a regular helix. There was still, however, no distortion of the extrudate surface. At higher flow rates, the flow lines began to "rupture" as the melt swirled violently into the inlet punctuated by alternating surges from the former relatively stagnant circulating corner flow regions which had not participated previously in the bulk flow. At the same time, the extrudate began to assume the shape of link-sausage as alternately smooth and grossly distorted sections emerged corresponding to the surges mentioned above. At still higher shear rates ($\Gamma > 3000$ sec⁻¹), the entrance flow completely broke down into random jets, resulting in a grossly distorted filament spurting from the capillary exit.

Some effects on flow patterns and extrudates were noted by varying the capillary length/diameter (L/D) ratio at constant wall shear rate. In the low-flow-rate stable-laminar-flow regime, the entrance angle seemed to decrease as the L/D ratio increased. In the unstable-flow regime, increasing the L/D ratio tended to damp out the disturbances in the melt and decrease the distortion of the extrudates. This latter effect has also been

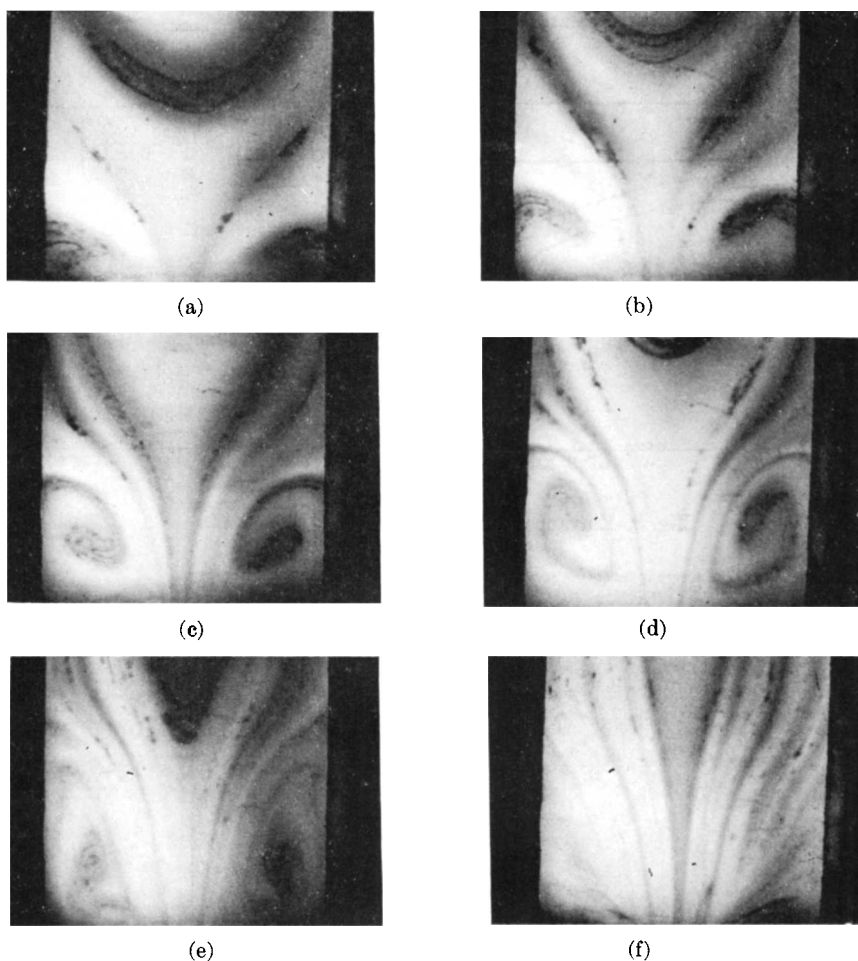


Fig. 4. Entrance flow patterns for low-density polyethylene for increasing capillary wall shear rate. Temperature in 180°C . (a) Shear rate = 6.9 sec^{-1} ; (b) shear rate = 17.3 sec^{-1} ; (c) shear rate = 33.9 sec^{-1} ; (d) shear rate = 65.5 sec^{-1} ; (e) shear rate = 294 unstable-intermediate stage; (f) shear rate = 561 sec^{-1} , unstable-later stage.

observed by earlier researchers. It would seem that the disturbances in the melt are being damped out within the capillary. This idea is supported by the experiments of Han and Lamonte²³ who have mounted transducers along the length of a capillary die and measured the signals in the unstable flow regime.

Polystyrene

At low flow rates, the melt streamlines seemed to move almost radially inward from the reservoir to the capillary (see Fig. 6). As the flow rate was increased, the bulk stream began to converge into the capillary at decreasing angles α of approach. Figure 5 plots α versus capillary wall

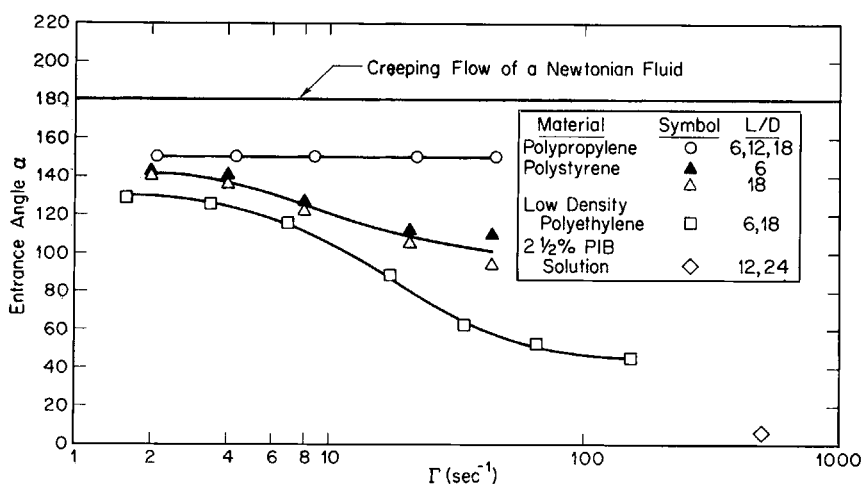
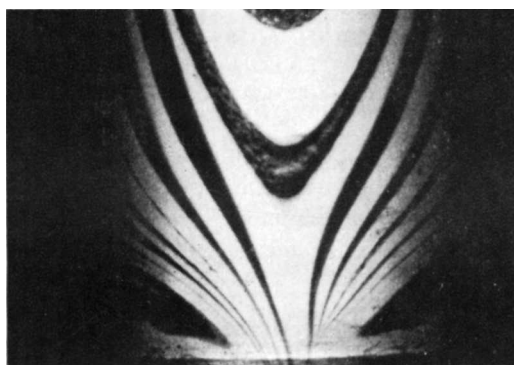


Fig. 5. Entrance angle as a function of shear rate.



(a)



(b)

Fig. 6. Entrance flow patterns for polystyrene for increasing capillary shear rate. Temperature is 180°C. (a) Shear rate = 8.0 sec⁻¹; (b) shear rate = 95.5 sec⁻¹ (spiralling instability).

shear rate. Again, a circulating torus-shaped region of melt remained in the corners of the reservoir above the die.

When the entrance angle α had decreased to above 90° (at a capillary wall shear rate between 44 and 96 sec^{-1}), a slight spiralling periodic oscillation was observed near the centerline. At this point, a smooth extrudate was still emerging from the capillary exit. When the flow rate was further increased, the swirling motion in the inlet became considerably more accentuated, and the emerging extrudate took on a helical appearance—indeed of a screw with a pitch about twice the diameter. Fluctuations in the pressure began to be observed.

Further increases in the flow rate caused massive “ruptures” of the flow lines and gross distortion of the extrudate which still maintained a general screw-like appearance. The circulating secondary flow region remained essentially distinct from the main stream. The pressure continued to fluctuate with greater amplitude. At shear rates above 900 sec^{-1} , the pulsations became still more violent and all order disappeared from the system, both upstream and downstream of the capillary. The flow in the die entrance became completely heterogeneous in the form of local velocities or “jets” of polymer “shooting” toward the capillary from random positions, including the former circulating flow regions as well as the wine glass stem. The extrudate became grossly distorted.

Again effects of length/diameter (L/D) ratio were observed. Increasing L/D ratio at constant capillary wall shear rate in the stable laminar-flow regime tended to decrease the angle of approach α in a more striking manner than with low-density polyethylene. In the unstable flow regime, increasing the L/D ratio seemed to have two effects. First, the overall flow behavior in the entrance seemed to be stabilized by increasing L/D . The circulating secondary flow regions seemed not to lose their identity. Secondly, increasing L/D damped out the disturbances in the melt and led to a smoother extrudate.

Polypropylene

The entrance flow patterns in this melt consisted of Newtonian-like radially inward streamlines (see Fig. 7). This persisted over the entire range of stable laminar flow. A smooth cylindrical extrudate emerged from the capillary. The constancy of the angle α with capillary wall shear rate is shown in Figure 5.

At capillary wall shear rates of $\sim 22 \text{ sec}^{-1}$, the emerging extrudate began to exhibit some roughness despite the fact that no instabilities were observed in the die entry. At higher flow rates ($> 45 \text{ sec}^{-1}$), a periodic oscillation began in the capillary inlet and the extrudate took on the shape of a regular helix, with the pitch increasing as the flow rate increased. Increasing the extrusion rate still further gave rise to a distinct swirling motion in the capillary inlet, which indeed almost resembled a tornado. The extrudate continued to take on an increasingly distorted shape, and

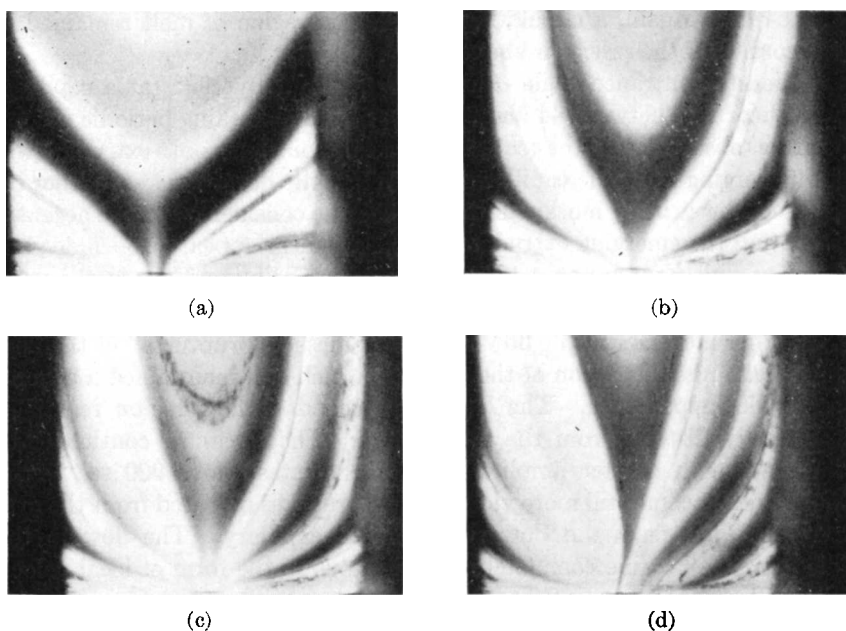


Fig. 7. Entrance flow patterns for isotactic polypropylene for increasing capillary shear rates. Temperature is 180°C. (a) Shear rate = 2.1 sec⁻¹; (b) shear rate = 22.1 sec⁻¹; (c) shear rate = 45.1 sec⁻¹; (d) shear rate = 236 sec⁻¹ (spiralling instability).

surface irregularities became more pronounced. (Compare the description of Bialas and White of this polymer.²)

Prints of a 16-mm color film showing the development of these flow patterns in the three melts are available by writing to one of us (JLW).

DISCUSSION

Laminar Flow

The first question which arises is how one might go about correlating the velocity fields in the capillary entrance with rheological properties of the melt. This is not as difficult a task as it may seem, for if we consider that polymer melts under the conditions studied are isotropic viscoelastic fluids in more or less creeping flow, we need only search the research literature in this area for solutions of the equations of force equilibrium and methods of dimensional analysis. This approach has been argued in our earlier papers,^{10,11} where it was pointed out that an analysis of creeping flow of viscoelastic fluids into a wedge and into a cone was carried out more than a decade ago by Langlois and Rivlin²⁴ who fully predicted the development of circulating secondary flows near the walls of the channel with increasing flow rate. (As shown by the combined experimental and theoretical studies of Giesekus,²⁵ spiralling flows are commonly observed to be superposed on shearing and other flows of polymer fluids.) This work²⁴ seems to have

been carried out at about the same time though completely independently of Tordella's low-density polyethylene experiments³ which we discussed earlier. Later treatments of this problem were given by Kaloni²⁶ and Murai and Mori.²⁷

Dimensional analysis methods for viscoelastic fluids have been similarly developed.²⁸⁻³¹ Application of these procedures yields the result that the dimensionless velocity field will be determined primarily by a dimensionless group of the form $\lambda_{ch}V/L$, where V is a characteristic velocity, L is a characteristic length, and λ_{ch} is a characteristic time. This group known as the Weissenberg number species the magnitude of the elastic memory and the ratio of the elastic forces to the viscous forces in the melt. There will also be a secondary influence by a series of other dimensionless groups known as viscoelastic ratio numbers, which, while representing the details of the non-Newtonian viscosity and the relaxation modulus function, do not contain kinematic parameters. As the entrance flow patterns may be specified by angle α , we may write:

$$\alpha = f_1 \left(\lambda_{ch} \frac{V}{L}, \text{viscoelastic ratio numbers, detailed geometry} \right). \quad (1)$$

A problem arises in expressing $\lambda_{ch}V/L$ as there is no exact definition of λ_{ch} . Rheologists have specified this quantity in different ways, e.g., the maximum relaxation time of linear viscoelasticity³⁰ and the ratio of normal stresses to shear stresses.²⁸ Now the principal normal stress difference measured at the well of a capillary is directly related to the capillary entrance pressure drop.^{21,22} The Weissenberg number is thus more or less equivalent to $\Delta p_e/\sigma_w$ which we have plotted as a function of capillary wall shear rate in Figure 3. We may now write

$$\alpha \sim f_2 \left(\frac{\Delta p_e}{\sigma_w}, \text{detailed geometry} \right). \quad (2)$$

In Figure 8, we have plotted all of our entrance angle data α as a function of $\Delta p_e/\sigma_w$. In addition, we have plotted data from some of our earlier experiments.¹¹ The data, as may be seen, correlate moderately well. We have attempted to fit various types of equations to these data. The best fit is of the form

$$\alpha = 178.5 (0.9644)^{\Delta p_e/\sigma_w} \text{ (degrees)} \quad (3)$$

or

$$\ln \left[\frac{\alpha}{178.5} \right] = -0.0362 \left(\frac{\Delta p_e}{\sigma_w} \right).$$

It is to be emphasized that this relationship is restricted to the particular geometry of the Instron rheometer. If the ratio of the diameter of the capillary to the barrel reservoir be changed, it should be expected that eq. (3) would no longer be valid. Indeed, we have found $\Delta p_e/\sigma_w$ to be a strong

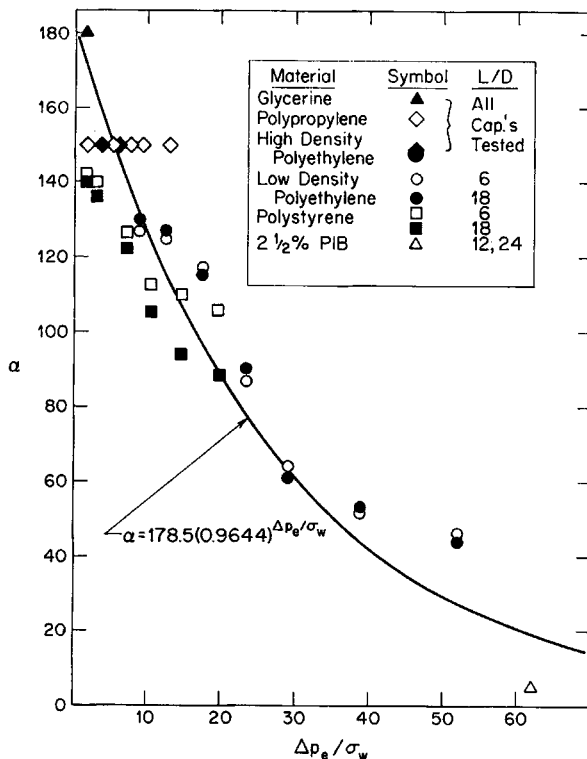


Fig. 8. Entrance angle as a function of $\Delta p_e / \sigma_w$.

function of this ratio. Related observations have been made by Schreiber³² and notably by Han and Kim.³³

Another point to discuss in the variation of flow patterns with capillary length/diameter ratio. This was observed in both polystyrene and low-density polyethylene. It is presumably due to the effect of pressure on rheological properties.

Instability

It was observed in each of the polymers studied in this paper as well as the polyisobutylene solution considered earlier^{10,11} that the first departure from laminar flow was seen as a swirling motion at the capillary inlet. In some of the melts, this seemed to be damped out in the reservoir, and indeed at first the spiralling motions were damped out in the capillary, and smooth extrudates appeared. (For the type of analysis required to predict extrudate distortion from entrance flow patterns, see White.³⁴) However, with increasing flow rates, the intensity of the spiralling increases and the extrudate begins to emerge in a helically distorted manner. At higher flow rates, gross fluctuations and apparent rupturing appear.

Although the spiralling instability seems to be common to all polymer fluids, the details of its occurrence differ. First, its duration during a se-

quence of shear rates seems to be inversely proportional to the elastic memory of the fluid. The interval of spiralling flow $\Delta\Gamma_{sp}$ seems to occur in increasing order of the polyisobutylene solutions, low-density polyethylene, polystyrene, polypropylene, and (apparently) high-density polyethylene, which corresponds more or less to the inverse order of elastic memory specified in an earlier paper by our group.¹¹

The question arises as to the mechanism of initiation of the spiralling disturbance. We are not able to satisfactorily answer this and indeed differ among ourselves. In any case, it may well be that there is a two-stage instability, first the spiralling and then the gross fluctuations which give rise to the major distortions of the extrudate at higher flow rates. These may be due to different mechanisms.

It is to be noted that for some years we have expected that the onset of the instability occurs at a critical value of the Weissenberg number.²³ Indeed, this was expected on the basis of earlier experimental results of Bagley³⁵ and Tordella.³⁶ However, the critical value of $\Delta p_e/\sigma_w$ observed varied from polymer to polymer.

CONCLUSIONS

A careful study of the development of flow patterns in polymer melts (low-density polyethylene, polystyrene, polypropylene) in the reservoir of a capillary rheometer has been carried out. In particular, at low flow rates, approximately radially inward flow to the capillary was observed. At higher flow rates, circulating secondary flows develop in the corners for the polyethylene and polystyrene, and a funnel-shaped entrance flow pattern with included angle α has been observed. This was correlated with the ratio of entrance pressure drop to wall shear stress, see Fig. 8 and eq. (3). At high extrusion rates, an instability occurs. It begins with a spiralling motion into the capillary which increases with intensity with increasing flow rate. Distorted extrudates with a helical form soon begin to appear. This observation seems to be generally true for a wide range of polymer fluids. At still higher flow rates, gross fluctuations and rupturing streamlines appear. This gives rise to highly distorted extrudates.

This research was supported in part by National Science Foundation Grant GK 2768. D. G. Salladay characterized the polystyrene sample. D. C. Bogue, J. W. Crowder, H. L. Davis, and G. E. Hagler made helpful comments throughout the course of this research.

References

1. J. Tordella, *J. Appl. Phys.*, **27**, 454 (1956); R. S. Spencer and R. E. Dillon, *J. Colloid. Sci.*, **4**, 241 (1949); J. J. Benbow and P. Lamb, *SPE Trans.*, **3**, 7 (1963); J. Tordella in *Rheology*, Vol. V, F. Eirich, Ed., Academic Press, New York, 1969.
2. G. A. Bialas and J. L. White, *Rubber Chem. Technol.*, **42**, 675, 682 (1969).
3. J. Tordella, *Trans. Soc. Rheol.*, **1**, 203 (1957).
4. H. Schott and W. Kaghan, *Ind. Eng. Chem.*, **51**, 844 (1959).
5. P. L. Clegg, in *Rheology of Elastomers* Mason and Wookey, Eds., Pergamon, New York, 1967.

6. E. B. Bagley and A. M. Birks, *J. Appl. Phys.*, **31**, 556 (1960).
7. H. Giesekus, *Rheol. Acta*, **7**, 127 (1968); *ibid.*, **8**, 411 (1969).
8. P. Schummer, *Rheol. Acta*, **6**, 192 (1967).
9. J. L. den Otter, *Plast. Polym.*, **38**, 155 (1970).
10. T. F. Ballenger and J. L. White, *Chem. Eng. Sci.*, **25**, 1191 (1970).
11. T. F. Ballenger, I. J. Chen, J. W. Crowder, G. Hagler, D. C. Bogue, and J. L. White, *Trans. Soc. Rheology*, **15**, 195 (1971).
12. H. L. Weissberg, *Phys. Fluids*, **5**, 1033 (1962); W. J. Harrison, *Proc. Camb. Phil. Soc.*, **19**, 307 (1919).
13. W. N. Bond, *Phil. Mag. (Ser. 6)* **50**, 1058 (1925); F. C. Johansen, *Proc. Roy. Soc., Ser. A*, **126**, 231 (1930).
14. H. P. Schreiber, E. B. Bagley, and A. M. Birks, *J. Appl. Polym. Sci.*, **4**, 241 (1960).
15. W. J. Roberts, Celanese Corp., personal communication, 1970.
16. A. B. Metzner, W. T. Houghton, R. A. Sailor, and J. L. White, *Trans. Soc. Rheol.*, **5**, 133 (1961).
17. R. Shinnar, personal communication, ca. 1965; M. Goldin, J. Yerushalmi, R. Pfeffer, and R. Shinnar, *J. Fluid Mech.*, **38**, 689 (1969).
18. T. F. Ballenger, M.S. Thesis in Chemical Engineering, University of Tennessee, Knoxville, 1971.
19. J. R. van Wazer, J. N. Lyons, K. Y. Kim, and R. E. Colwell, *Viscosity and Flow Measurement*, Interscience, New York, 1963.
20. A. B. Metzner, *A.I.Ch.E. J.*, **13**, 316 (1967).
21. H. L. LaNieve and D. C. Bogue, *J. Appl. Polym. Sci.*, **12**, 353 (1968).
22. D. P. Thomas and R. S. Hagan, *Polym. Eng. Sci.*, **9**, 164 (1969).
23. C. D. Han and R. R. Lamonte, to be published.
24. W. E. Langlois and R. S. Rivlin, Brown University Technical Report No. 3 to Office of Ordinance Research, U.S. Army Contract DA-19-020-ORD-4725, 1959; W. E. Langlois, Ph.D. Dissertation in Applied Mathematics, Brown University, 1957.
25. H. Giesekus, *Proc. 4th Int. Rheol. Cong.*, **1**, 249 (1963).
26. P. N. Kaloni, *J. Phys. Soc. Japan*, **20**, 132, 610 (1965).
27. R. Murai and Y. Mori, *J. Soc. Mat. Sci. Japan*, **15**, 354 (1966).
28. J. L. White, *J. Appl. Polym. Sci.*, **8**, 2339 (1964).
29. D. C. Bogue and J. Doughty, *Ind. Eng. Chem., Fundam.*, **5**, 243 (1966).
30. J. L. White and N. Tokita, *J. Appl. Polym. Sci.*, **11**, 321 (1967); A. B. Metzner, J. L. White, and M. M. Denn, *A.I.Ch.E.J.*, **12**, 863 (1966).
31. D. C. Bogue and J. L. White, NATO AGARDOGRAPH No. 144, 1970; J. L. White, *Rubber Chem. Technol.*, **42**, 257 (1969).
32. H. P. Schreiber, *Polym. Eng. Sci.*, **6**, 1 (1966).
33. C. D. Han and K. J. Kim, *Polym. Eng. Sci.*, in press.
34. J. L. White, *Rubber Chem. Technol.*, **42**, 691 (1969).
35. E. B. Bagley, *Trans. Soc. Rheol.*, **5**, 355 (1961).
36. J. Tordella, *J. Appl. Polym. Sci.*, **7**, 215 (1963).

Received March 22, 1971

Revised April 29, 1971